

Controllable and switchable chiral near-fields in symmetric graphene metasurfaces

Li Hu(胡莉), Hongxia Dai(代洪霞), Fayin Cheng(程发银), and Yuxia Tang(唐裕霞)

Citation: Chin. Phys. B, 2021, 30 (**12**): 127303. DOI: 10.1088/1674-1056/ac2e5d
Journal homepage: http://cpb.iphy.ac.cn; http://iopscience.iop.org/cpb

What follows is a list of articles you may be interested in

First-principles study of plasmons in doped graphene nanostructures

Xiao-Qin Shu(舒晓琴), Xin-Lu Cheng(程新路), Tong Liu(刘彤), and Hong Zhang(张红)
Chin. Phys. B, 2021, 30 (**9**): 097301. DOI: 10.1088/1674-1056/abe92d

Fabrication of sulfur-doped cove-edged graphene nanoribbons on Au(111)

Huan Yang(杨欢), Yixuan Gao(高艺璇), Wenhui Niu(牛雯慧), Xiao Chang(常霄), Li Huang(黄立), Junzhi Liu(刘俊治), Yiyong Mai(麦亦勇), Xinliang Feng(冯新亮), Shixuan Du(杜世萱), and Hong-Jun Gao(高鸿钧)
Chin. Phys. B, 2021, 30 (**7**): 077306. DOI: 10.1088/1674-1056/abfbd0

Correlated insulating phases in the twisted bilayer graphene

Yuan-Da Liao(廖元达), Xiao-Yan Xu(许霄琰), Zi-Yang Meng(孟子杨), and Jian Kang(康健)
Chin. Phys. B, 2021, 30 (**1**): 017305. DOI: 10.1088/1674-1056/abcfa3

Selective excitation of multipolar surface plasmon in a graphene-coated dielectric particle by Laguerre Gaussian beam

Yang Yang(杨阳), Guanghua Zhang(张光华), Xiaoyu Dai(戴小玉)
Chin. Phys. B, 2020, 29 (**5**): 057302. DOI: 10.1088/1674-1056/ab7e97

Optical binding forces between plasmonic nanocubes：A numerical study based on discrete-dipole approximation

Zhang Xiao-Ming, Xiao Jun-Jun, Zhang Qiang
Chin. Phys. B, 2014, 23 (**1**): 017302. DOI: 10.1088/1674-1056/23/1/017302

Controllable and switchable chiral near-fields in symmetric graphene metasurfaces*

Li Hu(胡莉)[1,2,†], Hongxia Dai(代洪霞)[1,2], Fayin Cheng(程发银)[1,2], and Yuxia Tang(唐裕霞)[1,3]

[1] *Chongqing Key Laboratory of Intelligent Perception and BlockChain Technology, Chongqing Technology and Business University, Chongqing* 400067, *China*

[2] *Department of Applied Physics, School of Computer Science and Information Engineering, Chongqing Technology and Business University, Chongqing* 400067, *China*

[3] *Soft Matter and Interdisciplinary Research Center, College of Physics, Chongqing University, Chongqing* 400044, *China*

(Received 21 August 2021; revised manuscript received 27 September 2021; accepted manuscript online 11 October 2021)

A strong chiral near-field plays significant roles in the detection, separation and sensing of chiral molecules. In this paper, a simple and symmetric metasurface is proposed to generate strong chiral near-fields with both circularly polarized light and linearly polarized light illuminations in the mid-infrared region. Owing to the near-field interaction between plasmonic resonant modes of two nanosheets excited by circularly polarized light, there is a strong single-handed chiral near-field in the gap between the two graphene nanosheets and the maximum enhancement of the optical chirality could reach two orders of magnitude. As expected, the intensity and the response wavelength of the chiral near-fields could be controlled by the Fermi level and geometrical parameters of the graphene nanosheets, as well as the permittivity of the substrate. Meanwhile, based on the interaction between the incident field and scattered field, the one-handed chiral near-field in the gap also could be generated by the linearly polarized light excitation. For the two cases, the handedness of the chiral near-field could be switched by the polarized direction of the incident light. These results have potential opportunities for applications in molecular detection and sensing.

Keywords: plasmonic resonance, chiral near-field, graphene, metasurface

PACS: 73.20.Mf, 25.70.Ef, 78.67.Wj **DOI:** 10.1088/1674-1056/ac2e5d

1. Introduction

Chirality is a geometric property of objects, which indicates that the objects could not overlap with their mirror images through simple translations or rotations. There are a lot of chiral molecules in nature, for instance, proteins, DNA, nucleic acids, and so on.[1,2] Because chiral molecules with the opposite handedness generally show different behaviors in biological processes, the recognition and discrimination of chiral molecules are extremely important in analytical chemistry, biology and pharmacology.[3,4] Nevertheless, the chiral response of natural molecules is very weak and occurs in the ultraviolet region, which hampers their further applications.

In recent years, owing to the excellent properties of the light confinement and local field enhancement, plasmonic nanostructures have drawn a lot of attention owing to their potential applications in light absorption, Raman scattering, chiral response, etc.[5–10] Based on the plasmonic resonance, various metamaterials have been proposed to enhance chiral responses in both the far-field and near-field.[11–14] Especially, the chiral near-field has attracted a lot of interest due to its wide applications, such as molecular recognition, detection, separation, and sensing,[15–18] which are expected with the excellent properties of enough strength, single handedness, large area, etc. Utilizing the plasmonic resonance of metal materials, strong chiral near-fields have been obtained in the visible and near-infrared regions with various chiral and achiral nanostructures.[19–23] In order to obtain chiral responses in the mid-infrared region, graphene is considered to be the best alternative material, because doped graphene nanostructures show strong plasmonic resonances with a relatively low loss. Meanwhile, graphene nanostructures could be accurately fabricated and transferred to various substrates and the plasmonic resonance could be controlled by chemical doping and electrical doping.[24–28] In addition, the twisted bilayer graphene also has chiral properties.[29–31] Therefore, many graphene and graphene-based nanostructures have been designed to generate strong chiral responses.[25,32–35] For example, Kong *et al.* obtained giant circular dichroic (CD) responses with chiral graphene assemblies;[26] Wang *et al.* designed the achiral metal-nanorods with graphene-nanobelt arrays to achieve CD signals;[36] Fu *et al.* proposed an achiral nanoring to achieve chiral near-field;[25] chiral near-field also had been achieved with twisted bilayer graphene.[37] For the studies of chiral near-fields, most of them are either complex in structures, or the chiral fields are both left- and right-handed, or the response area is small. As a result, achieving a strong uniform chiral near-field in the mid-infrared region still presents a challenge.

*Project supported by the National Natural Science Foundation of China (Grant No. 11804035) and Science and Technology Research Program of Chongqing Municipal Education Commission, China (Grant No. KJ1706153).

†Corresponding author. E-mail: huli@ctbu.edu.cn

© 2021 Chinese Physical Society and IOP Publishing Ltd

In this work, a graphene metasurface, composed of two same nanosheets in a unit cell, is proposed to produce strong and uniform superchiral fields with both circularly polarized light (CPL) and linearly polarized light (LPL) illuminations. With the metasurface, a one-handed chiral near-field is achieved in the gap of two graphene nanosheets, which could be controlled by the Fermi level of the graphene sheets and the other parameters, and whose handedness could be controlled by the wavelength and the polarization direction of the incident light. To understand the physical mechanism generating the uniform chiral near-field, the distributions of electric and magnetic fields are analyzed.

2. Method and model of simulation

In order to achieve enhanced single-handed near-fields at the mid-infrared region with easily prepared nanostructures, here, we proposed a graphene metasurface composed of single-layer graphene arrays with a symmetric nanosheet-dimer in each unit cell on the substrate, as shown in Figs. 1(a) and 1(b). The graphene arrays are located on the x–y plane and the exciting light is propagated along the z-axis. The array is a periodic structure with a fixed period of 300 nm both in x- and y-directions. The side length $a = b = 80$ nm, and the distance of the gap between the two nanosheets is set as g. The monolayer graphene is deposited on the low resistivity Si substrate ($\varepsilon_s = 12.04$) and the whole nanostructure is placed in the air $\varepsilon_m = 1$. The single-layer graphene nanosheets could be characterized by the surface conductivity σ_s, which is a function of the frequency of the exciting light and involves contributions from inter- and intra-band transitions,[34]

$$\sigma_s = \sigma_{inter} + \sigma_{intra}, \tag{1}$$

$$\sigma_{inter} = \frac{e^2}{4\hbar}\left[\frac{1}{2} + \frac{1}{\pi}\arctan\frac{\hbar\omega - 2E_f}{2k_BT} - \frac{i}{2}\ln\frac{(\hbar\omega - 2E_f)^2}{(\hbar\omega - 2E_f)^2 + (2k_BT)^2}\right], \tag{2}$$

$$\sigma_{intra} = -i\frac{e^2 k_B T}{\pi(\omega - i\tau^{-1})} \times \left[\frac{E_f}{k_BT} + 2\ln\left(\exp\left(-\frac{E_f}{k_BT}\right) + 1\right)\right], \tag{3}$$

where e, $\hbar$, k_B, E_f, T, and τ are the electron charge, reduced Planck's constant, Boltzmann's constant, Fermi level of graphene, temperature ($T = 300$ K), and carrier relaxation time, respectively. Here, $\tau = \mu E_f / e v_f^2$, μ (10000 cm^2/(V·s)) is the moderate carrier mobility, v_f (10^6 m/s) is the Fermi velocity, and the angular frequency of the stimulating light is $\omega = 2\pi c/\lambda$ (λ is the incident wavelength of light in the vacuum; c is the speed of light in the vacuum). The thickness of the monolayer graphene sheets is set as $t_g = 1$ nm. So, the equivalent relative permittivity of the graphene could be expressed as

$$\varepsilon_g = 1 + \frac{i\sigma_s}{\omega\varepsilon_0 t_g}, \tag{4}$$

where ε_0 is the permittivity of the vacuum. The sample is easy to prepare in practice. The monolayer graphene grown on copper foil by chemical vapor deposition (CVD) could be repeatedly transferred to the predefined position on the substrate.

Here, to quantify the chiral near-fields, the optical chirality C is used,[38]

$$C \equiv \frac{\varepsilon_0}{2}\boldsymbol{E}\cdot\nabla\times\boldsymbol{E} + \frac{1}{2\mu_0}\boldsymbol{B}\cdot\nabla\times\boldsymbol{B}, \tag{5}$$

where $\boldsymbol{E}$ and $\boldsymbol{B}$ are the electric and magnetic fields, and μ_0 is the permeability of the vacuum. Further, to calculate the optical chirality, a simpler version of C is deduced as

$$C = -\frac{\varepsilon_0\omega}{2}\mathrm{Im}(\boldsymbol{E}^*\cdot\boldsymbol{B}). \tag{6}$$

The enhancement of the optical chirality could be calculated by

$$\hat{C} = C/\left|C_{CPL}^{\pm}\right|, \tag{7}$$

where $C_{CPL}^{\pm} = \pm\frac{\varepsilon_0\omega}{2c}|\boldsymbol{E}|^2$ is the maximum optical chirality illuminated with the left-handed and right-handed circularly polarized light (LCP (+) and RCP (−)) without any nanostructure. The absorption spectra are expressed as $A = 1 - R - T$, where T and R are the transmittance and reflectance of the nanostructures, respectively. In this work, all the electromagnetic responses of the graphene metasurface were simulated with the finite element method (FEM) software (COMSOL Multiphysics). In simulations, we used the periodic boundary conditions at the x and y directions and the perfectly matched layer (PML) at the top and bottom of the structures. Meanwhile, nonuniform meshes were used for formatting the object, and the largest mesh was set less than $\lambda/10$. The maximum mesh in the gap between two graphene nanosheets was set less than 1 nm.

3. Results and discussion

As depicted in Fig. 1(c), when the metasurface is stimulated with CPL along the z-direction, there are two strong resonance peaks in the mid-infrared region. From the distributions of surface charge density of graphene nanosheets excited with LCP at resonant wavelengths (the inset of Fig. 1(c)), it could be seen that there are a longitudinal coupling mode ($\lambda =$ 18.4 μm) and a transverse coupling mode ($\lambda = 16.25$ μm) of the two graphene nanosheets. Due to the geometrical symmetry of the metasurface, the absorption spectra coincide with each other with the LCP and RCP illuminations, which results in a zero CD response. However, owing to the near-field interaction between different plasmonic modes

of metamolecules,[39] the chiral near-field properties are extremely different in the two cases. To calculate the enhancement of the chiral near-fields and well mimic the real experiment, the volume-averaged optical chirality enhancement in the gap between the two nanosheets is calculated, which is defined as $\langle \hat{C} \rangle = \frac{1}{V} \int_V \hat{C} \cdot \mathrm{d}V$. As shown in Fig. 1(d), there are four peaks in the averaged optical chirality spectra and the chirality is just opposite for the incident light with opposite polarization (LCP and RCP). Meanwhile, for any polarized light, the handedness of the chiral near-field also could be switched by changing the wavelength of the exciting light. Especially, it could be seen that the absolute value of the averaged optical chirality enhancement is about 50 times at the peaks (peaks I and II in Fig. 1(d)) of the longer wavelengths, which is much larger than that of some reported graphene-based nanostructures. In contrast, the chiral responses in the shorter wavelengths are very weak, so, we mainly focus on the chiral properties at the longer wavelengths in the following.

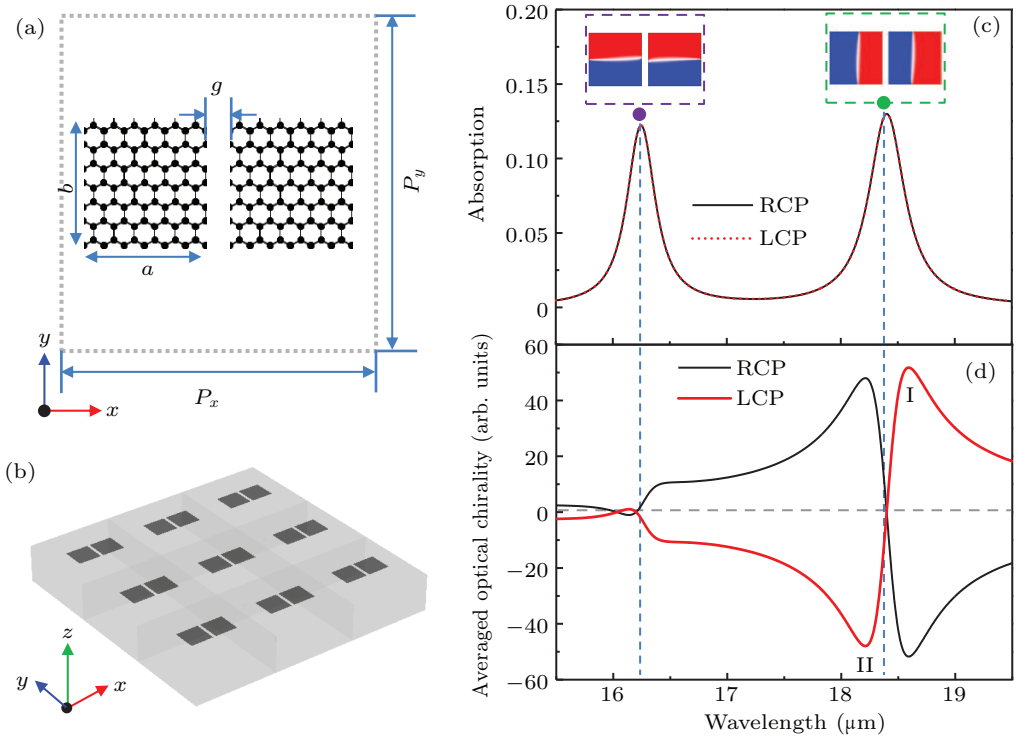


Fig. 1. (a) Top view of a unit cell of graphene metasurfaces with structural parameters. (b) 3D schematic of the graphene metasurface. (c) Absorption spectra of the metasurface stimulated with RCP (black solid line) and LCP (red dot line). Inset: the distributions of surface charge density of graphene nanosheets excited with LCP at two resonance wavelengths (purple dot: 16.25 μm, green dot: 18.4 μm). (d) Averaged optical chirality enhancement spectra of the gap between two graphene nanosheets stimulated with RCP (black line) and LCP (red line). Here $P_x = P_y = 300$ nm, $a = b = 80$ nm, $t_g = 1$ nm, $g = 10$ nm, $E_f = 0.6$ eV, and $T = 300$ K.

To achieve a deep understanding of the physical mechanism of the chiral near-field response, the near-field maps of the metasurface are simulated. Owing to the symmetric properties of chiral responses with LCP and RCP illuminations, here, we only discuss the near-field properties excited by LCP. As depicted in Figs. 2(a) and 2(b), when the incident wavelength is 18.4 μm (the wavelength of the resonance peak), the enhancements of the electric field and magnetic field are stronger than those of the others (18.2 μm: chiral peak II; 18.6 μm: chiral peak I, as shown in Fig. 1(d)). For the three scenarios (the wavelengths of the incident light are 18.2 μm (i), 18.4 μm (ii) and 18.6 μm (iii), respectively), the strongest enhancements of the magnetic fields occur on both sides of the graphene nanosheets (Fig. 2(a)), but the strongest enhancements of the electric fields are distributed in the gap between the two graphene pieces (Fig. 2(b)). Accordingly, there are chiral near-field responses around the graphene sheets illuminated with the three wavelengths. However, extremely different from the distributions of the electric and magnetic fields, the chiral near-field enhancements in the gap between the two graphene pieces are obviously enhanced at 18.2 μm (Fig. 2(c)-i) and 18.6 μm (Fig. 2(c)-iii), which could be up to two orders of magnitude, but nearly vanish at 18.4 μm (Fig. 2(c)-ii). Meanwhile, the handedness of the chiral near-fields in the gap is uniform and just opposite for 18.2 μm and 18.6 μm (Figs. 2(c)-i and 2(c)-iii), which is very important in applications of chiral separation, sensing, etc.

Therefore, we mainly focus on the chiral near-field between two graphene nanosheets in this work (just as Fig. 1(d)). To further explain the chiral flip, the components of the electric field and magnetic field are calculated with the illuminations of 18.2 μm, 18.4 μm, and 18.6 μm, respectively. As shown in Figs. 3 and 4, the components of the electric fields are consistent and the magnetic fields are exactly opposite for 18.2 μm

and 18.6 μm, which just lead to the opposite handedness of the chiral near-fields owing to $C \propto \mathrm{Im}(\boldsymbol{E}^* \cdot \boldsymbol{B})$. Therefore, we could achieve extremely enhanced single-handed near-fields and the handedness could be tuned by the wavelength and the polarization of the exciting light with the symmetric metasurface.

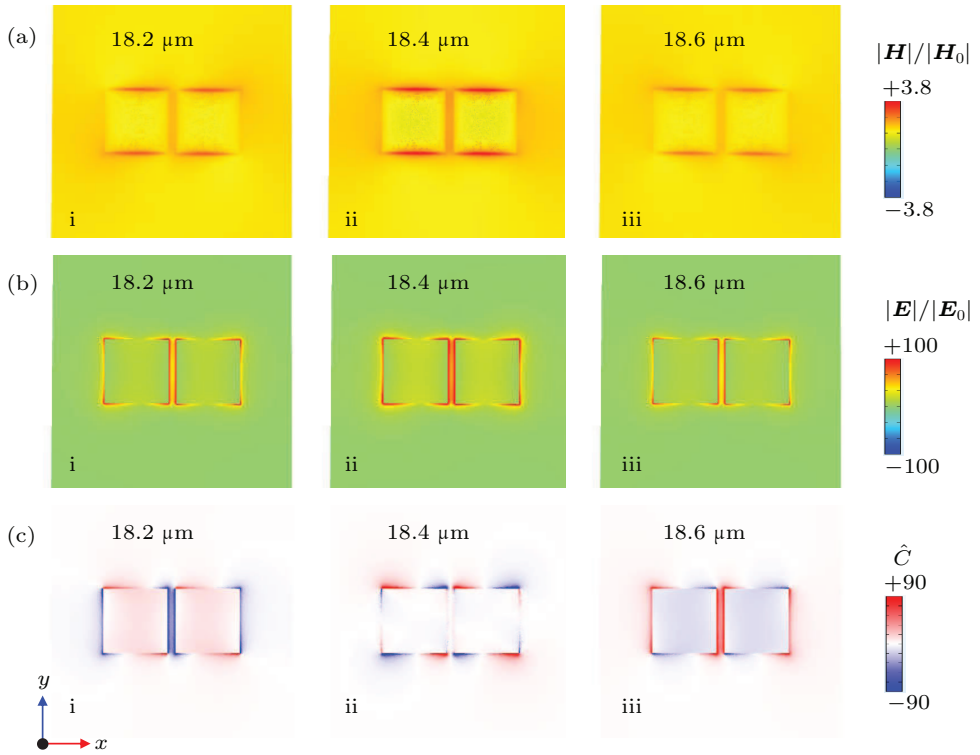


Fig. 2. The 2D maps of the enhancement of magnetic field (a), electric field (b) and optical chirality (c) in a unit cell at the x–y plane of graphene metasurfaces excited by LCP with the wavelength 18.2 μm (i), 18.4 μm (ii) and 18.6 μm (iii). The x–y slices are cut from the middle position of the graphene nanosheets. $\boldsymbol{H}_0$ and $\boldsymbol{E}_0$ are the incident magnetic and electric fields.

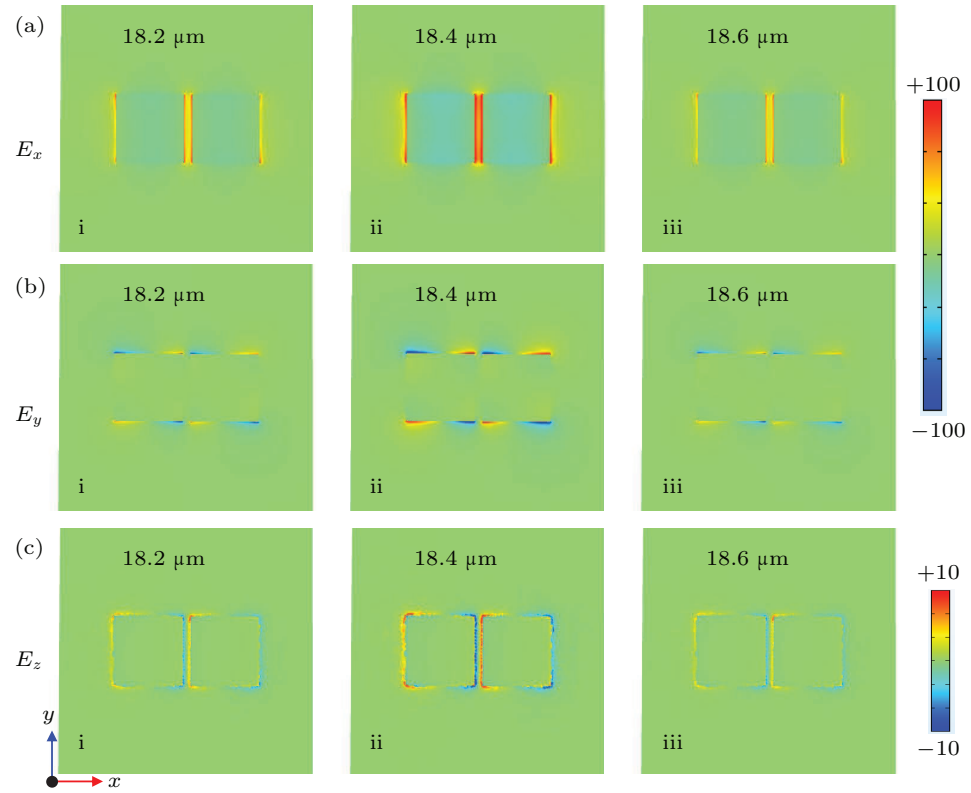


Fig. 3. The x-components (a), y-components (b) and z-components (c) of electric field maps of an unit cell excited with LCP at the wavelength of 18.2 μm (i), 18.4 μm (ii) and 18.6 μm (iii). The x–y slices are cut from the middle position of the graphene sheets.

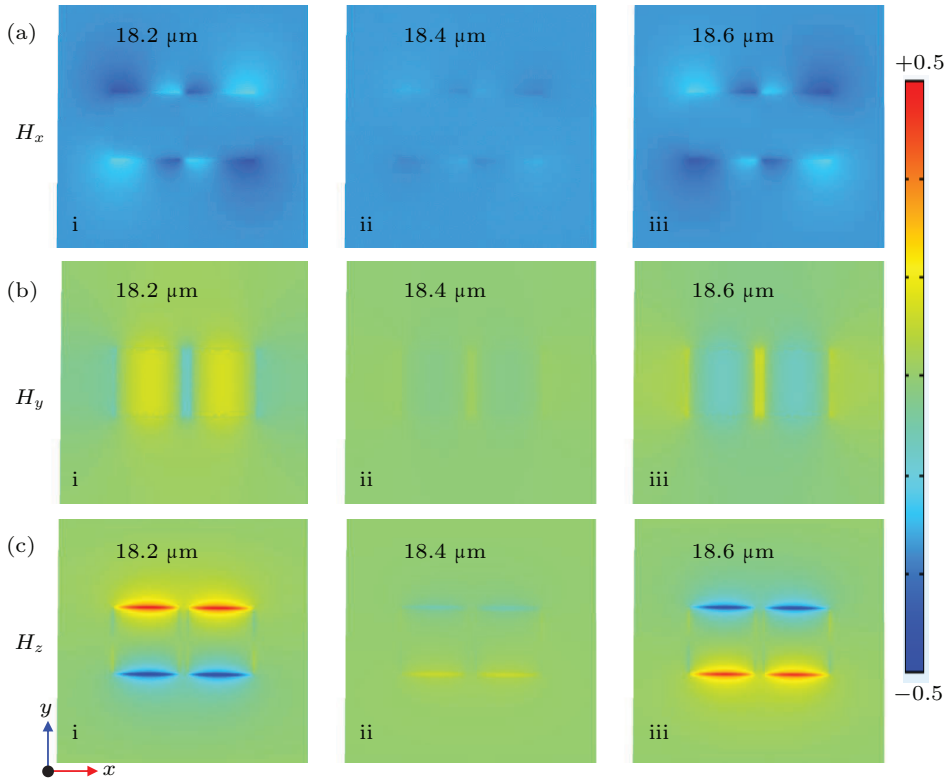


Fig. 4. The x-components (a), y-components (b) and z-components (c) of magnetic field maps of an unit cell excited with LCP at the wavelength of 18.2 μm (i), 18.4 μm (ii) and 18.6 μm (iii). The x–y slices are cut from the middle position of the graphene sheets.

It is well known that the Fermi level of graphene plays an important role in plasmonic resonances, here, for the graphene nanosheets, it could be controlled via chemical doping. To illustrate its influence on the chiral near-field in the gap, here, we change the Fermi level from 0.6 eV to 0.9 eV and the other parameters remain unchanged. As shown in Fig. 5(a), with the increase of the Fermi level, the averaged optical chirality enhancement of the gap between the two nanosheets increases and the peak position shows a blue shift, which is because of the blue shift of the plasmonic resonance peaks ($\lambda \propto \frac{\hbar^2 c^2}{4\pi e^2 E_f}$),[36] as shown in Fig. S1a (supporting information). Therefore, we could control the wavelength and the strength of the chiral near-field in the gap by changing the Fermi level.

As discussed above, the area of chiral near-fields is important in applications such as chiral detection and sensing, here, it could be adjusted by the distance between two nanosheets. Meanwhile, the coupling effect between two metamolecules depends on the distance between the metamolecules. Based on these, it is necessary to discuss the dependence of chiral near-fields on the distance between two nanosheets. As shown in Fig. S1b (supporting information), with the distance (g) increasing from 10 nm to 25 nm and the other parameters keeping the same as those in Fig. 1, the resonant peak of the longer wavelength blue shifts. Correspondingly, the peak (at the longer wavelength) of the averaged optical chirality enhancement blue shifts and the strength decreases (Fig. 5(b)), which is a result of the decrease of the coupling effect between the two graphene nanosheets. Thus, in applications, the area and the strength of the single-handed near-field could be controlled by changing the distance between the two nanosheets.

Besides the gap, the other parameters also affect the response of chiral near-fields. As we all know, the size of plasmonic structures has an influence on plasmonic resonances. When we change the side lengths (a and b, $a = b$) from 60 nm to 80 nm and fix the other parameters as those in Fig. 1, the resonant peak red shifts and their strength increases, as shown in Fig. S1c (supporting information). However, for the averaged optical chirality enhancement in the gap between the two graphene sheets, as shown in Fig. 5(c), the peak of the chiral response red shifts but the strength stays roughly the same with the increase of the side lengths. Meanwhile, the substrate material plays an important role on plasmonic resonances. When the permittivity of the substrate (ε_s) changes from 8 to 14, and the other parameters remain unchanged, the resonant peak red shifts and the strength decreases (Fig. S1d (supporting information)), which further results in a similar change for the chiral near-field response of the gap (Fig. 5(d)). Therefore, we could adjust different parameters to meet the requests of different applications.

As it has been shown in many studies, owing to the interaction between the incident field and scattered field, the chiral

near-field could be achieved in symmetric nanostructures excited with LPL at normal incident.[19,21,40,41] In light of this, here, we also study the chiral near-field of the symmetric metasurface with LPL illuminations at two polarized directions, as shown in Fig. 6(a). For simplicity, we denote the two polarization cases of LPL with ① and ②. Here, ① means the polarization direction along the diagonal of the positive x-axis and the positive y-axis, and ② means the polarization direction along the diagonal of the positive x-axis and the negative y-axis. As that of illuminated with CPL, due to the coupling effect between the two nanosheets, there are two resonance peaks ($\lambda = 16.25$ μm, 18.4 μm) illuminated with LPL both ① and ②, which coincide with each other, as shown in Fig. 6(b). As expected, but different from that of illuminated with CPL, there is a pronounced enhancement of the volume-averaged optical chirality in the gap between the two sheets at the plasmonic resonant peak ($\lambda = 18.4$ μm) and the handedness of the chiral near-fields is just opposite with two polarizations of ① and ②, as shown in Fig. 6(c). When the metasurface is excited with $\lambda = 18.4$ μm, similar to that of excited with CPL, the strongest enhancements of magnetic fields (Fig. 6(d)) and electric fields (Fig. 6(e)) are distributed at different districts, and the maximum uniform enhancement of the chiral near-fields (Fig. 6(f)) still occurs in the gap between the two nanosheets.

Similarly, the plasmonic resonance and chiral near-field could be tuned by the Fermi level of graphene and the other parameters with LPL illumination. For comparison, we change one parameter every time and the others remain the same as those in Fig. 1. The plasmonic resonances change with the variable parameters, as shown in Fig. S2 (supporting information). For the chiral near-field in the gap between the two graphene nanosheets, as shown in Fig. 7(a), with the increase of the Fermi level, the chiral response enhances and the response wavelength has a blue shift. When the gap between the two nanosheets enlarges, the chiral response obviously decreases and the wavelength blue shifts (Fig. 7(b)). The wavelength of the chiral response red shifts but the strength change little with the side length (a and b) increasing (Fig. 7(c)). With the increase of the permittivity of the substrate, the chiral response gradually decreases and the wavelength red shifts (Fig. 7(d)). Therefore, we can also tune the wavelength and strength of chiral near-field response by Fermi levels and various structural parameters in different applications with LPL illumination.

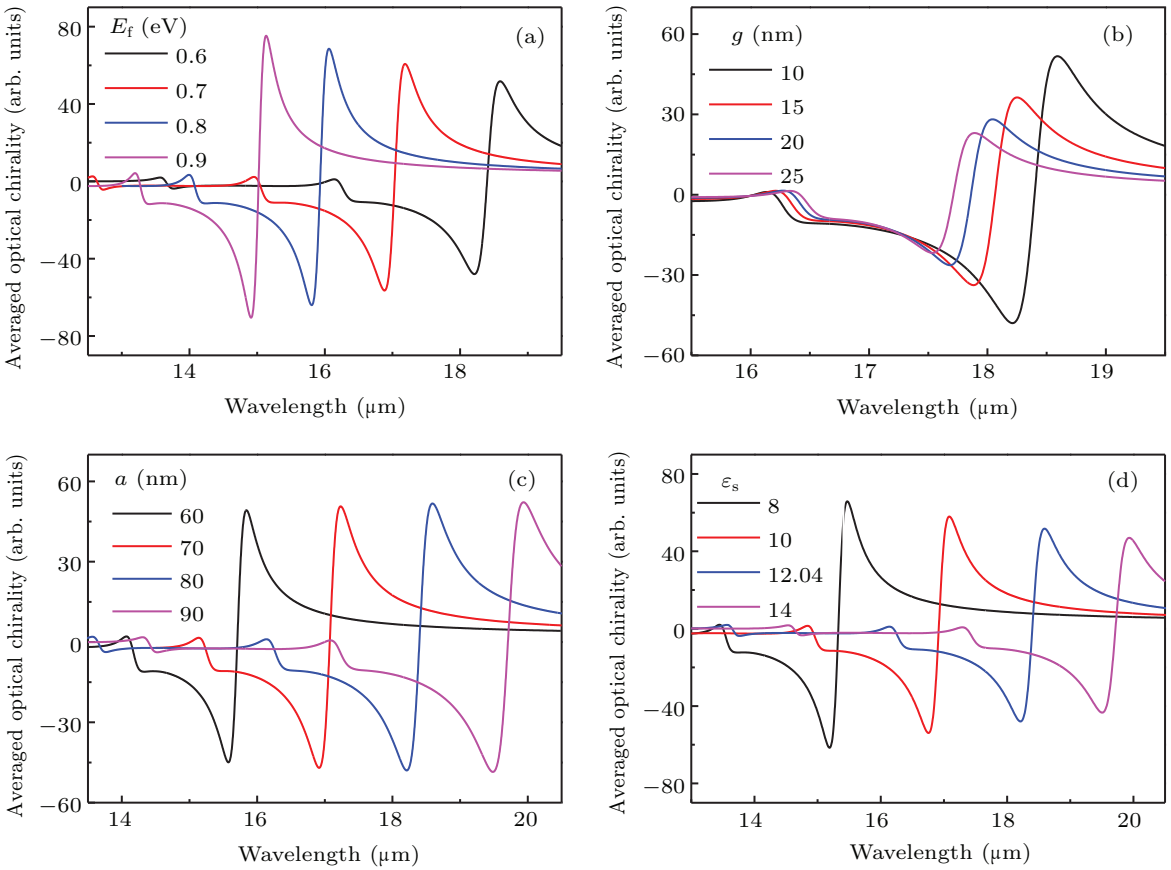


Fig. 5. Averaged optical chirality enhancement spectra of the gap between two graphene nanosheets of the graphene metasurface with different Fermi levels (a); different gaps (b); different side lengths (c) and different permittivity of substrates (d) excited by CPL. The other parameters are the same as those in Fig. 1.

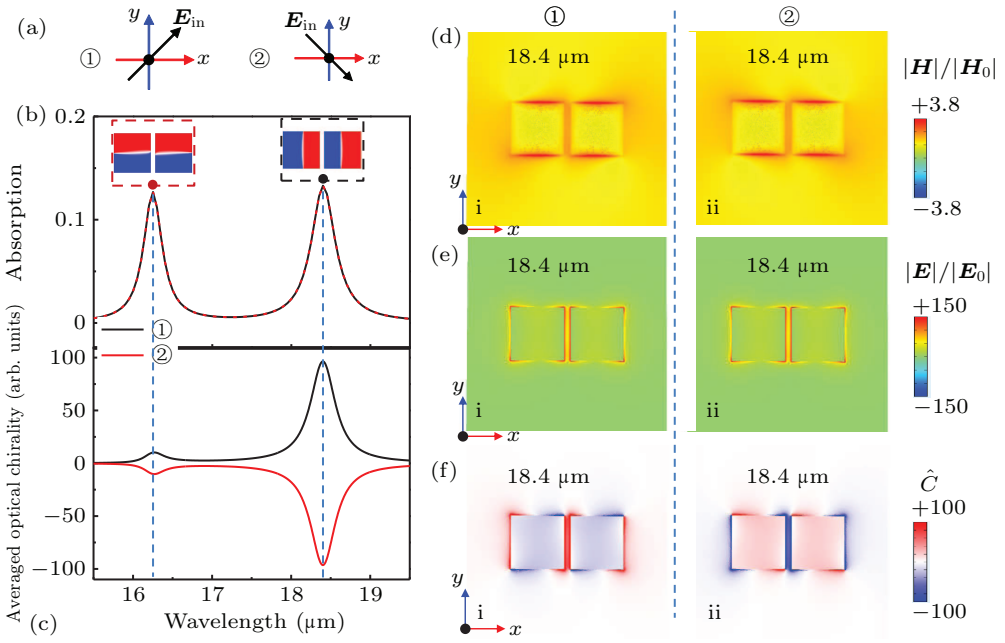


Fig. 6. (a) Schematic of the polarized direction of the incident electric field, ① represents the incident electric field along the diagonal of $+x$ and $+y$ directions and ② means the incident electric field along the diagonal of $+x$ and $-y$ directions. (b) The absorption spectra of the graphene metasurface excited with linear polarized light. The insets show the surface charge distributions of graphene sheets at resonance peaks. (c) The averaged optical chirality enhancement spectra in the gap between two graphene sheets excited with LPL. Black lines: the polarized direction as shown in ①; red lines: the polarized direction as shown in ②. The 2D maps of the enhancement of magnetic field (d), electric field (e) and optical chirality (f) in a unit cell at the x–y plane of the graphene metasurface excited by LPL at 18.4μm. i: the polarized direction of LPL as shown in ①; ii: the polarized direction of LPL as shown in ②. The x–y slices are cut from the middle position of the graphene nanosheets. $\boldsymbol{H}_0$ and $\boldsymbol{E}_0$ are the incident magnetic and electric fields. All parameters are the same as those in Fig. 1.

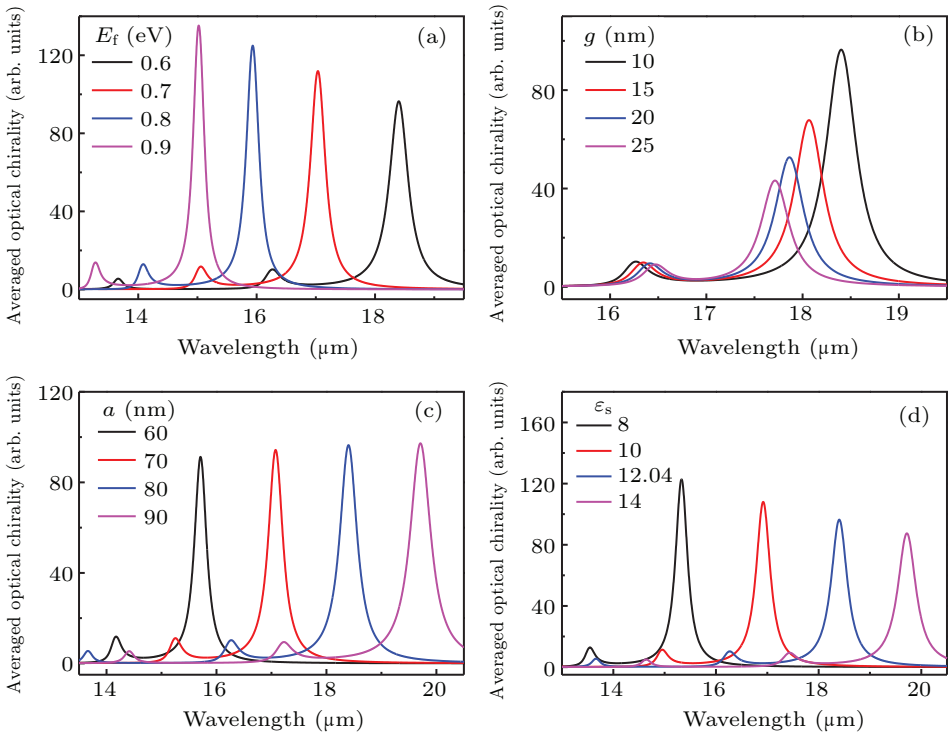


Fig. 7. Averaged optical chirality enhancement spectra of the gap between two graphene nanosheets of the graphene metasurface with different Fermi levels (a); different gaps (b); different side lengths (c) and different permittivity of substrates (d) excited by LPL (Fig. 6(a)-①). The other parameters are the same as those in Fig. 1.

4. Conclusion

In summary, a graphene metasurface with a symmetrical structure is proposed to generate strong chiral near-fields with both CPL and LPL illuminations. Owing to the near-field interaction between different plasmonic modes excited by CPL, a strong single-handed near-field is obtained in the gap between the two nanosheets. With the increase of the Fermi level, the peaks in the averaged optical chirality enhancement

spectrum blue shift and the intensities increase. With the distance of the two nanosheets increasing, the area increases but the strength of the chiral near-field in the gap decreases. Meanwhile, the response of the chiral near-field in the gap is influenced by the size of graphene and the permittivity of the substrate. On the other hand, based on the interaction between the incident field and scattered field, one-handed chiral fields could be obtained in the same district with the LPL illumination. Especially, all the handedness of chiral near-fields could be switched by the polarization of the incident light. Thus, the simple graphene metasurface could be used in the detection, sensing and separation of chiral molecules.

References

[1] Cecconello A, Besteiro L V, Govorov A O and Willner I 2017 *Nat. Rev. Mater.* **2** 17039
[2] Luo Y, Chi C, Jiang M, Li R, Zu S, Li Y and Fang Z 2017 *Adv. Opt. Mater.* **5** 1700040
[3] Hao C, Xu L, Kuang H and Xu C 2020 *Adv. Mater.* **32** 1802075
[4] Matuschek M, Singh D P, Jeong H H, Nesterov M, Weiss T, Fischer P, Neubrech F and Liu N 2018 *Small* **14** 1702990
[5] Collins J T, Kuppe C, Hooper D C, Sibilia C, Centini M and Valev V K 2017 *Adv. Opt. Mater.* **5** 1700182
[6] Wang X and Tang Z 2017 *Small* **13** 1601115
[7] Ben-Moshe A, Maoz B M, Govorov A O and Markovich G 2013 *Chem. Soc. Rev.* **42** 7028
[8] Chen Y, Cheng Y and Sun M 2021 *J. Phys. Chem. C* **125** 21301
[9] Mu X, Hu L, Cheng Y, Fang Y and Sun M 2021 *Nanoscale* **13** 581
[10] Cui L, R Li, Mu T, Wang J, Zhang W and Sun M 2021 *Spectrochimica Acta Part A: Molecular and Biomolecular Spectroscopy* **264** 120283
[11] Kong X T, Khosravi Khorashad L, Wang Z and Govorov A O 2018 *Nano Lett.* **18** 2001
[12] Kuzyk A, Schreiber R, Fan Z, Pardatscher G, Roller E M, Hogele A, Simmel F C, Govorov A O and Liedl T 2012 *Nature* **483** 311
[13] Fan Z and Govorov A O 2010 *Nano Lett.* **10** 2580
[14] Kang L, Ren Q and Werner D H 2017 *ACS Photon.* **4** 1298
[15] Hendry E, Carpy T, Johnston J, Popland M, Mikhaylovskiy R V, Lapthorn A J, Kelly S M, Barron L D, Gadegaard N and Kadodwala M 2010 *Nat. Nanotechnol.* **5** 783
[16] Meinzer N, Hendry E and Barnes W L 2013 *Phys. Rev. B* **88** 041407
[17] Shi Y, Zhu T, Zhang T, Mazzulla A, Tsai D P, Ding W, Liu A Q, Cipparrone G, Saenz J J and Qiu C W 2020 *Light Sci. Appl.* **9** 62
[18] Lee Y Y, Kim R M, Im S W, Balamurugan M and Nam K T 2020 *Nanoscale* **12** 58
[19] Tian X, Fang Y and Sun M 2015 *Sci. Rep.* **5** 17534
[20] Davis T J and Hendry E 2013 *Phys. Rev. B* **87** 085405
[21] Hu L, Dai H, Xi F and Long T 2018 *Euro. Phys. J. D* **72** 201
[22] Schäferling M, Engheta N, Giessen H and Weiss T 2016 *ACS Photon.* **3** 1076
[23] Schäferling M, Dregely D, Hentschel M and Giessen H 2012 *Phys. Rev. X* **2** 031010
[24] Huang Y, Yao Z, Hu F, Liu C, Yu L, Jin Y and Xu X 2017 *Carbon* **119** 305
[25] Fu T, Chen Y, Wang T, Li H, Zhang Z and Wang L 2017 *Opt. Express* **25** 24623
[26] Kong X T, Zhao R, Wang Z and Govorov A O 2017 *Nano Lett.* **17** 5099
[27] Xiao S, Wang T, Liu T, Zhou C, Jiang X and Zhang J 2020 *J. Phys. D: Appl. Phys.* **53** 503002
[28] Cui L and Sun M 2021 *J. Phys. Chem. C* **125** 22370
[29] Mu X and Sun M 2020 *Materials Today Physics* **14** 100222
[30] Cui L, Wang J and Sun M 2021 *Reviews in Physics* **6** 100054
[31] Stauber T, Low T and Gomez-Santos G 2018 *Phys. Rev. Lett.* **120** 046801
[32] Shi C, He X, Peng J, Xiao G, Liu F, Lin F and Zhang H 2019 *Optics and Laser Technology* **114** 28
[33] Ye L, Zeng F, Zhang Y and Liu Q H 2019 *Carbon* **148** 317
[34] Zhou S, Lai P, Dong G, Li P, Li Y, Zhu Z, Guan C and Shi J 2019 *Opt. Express* **27** 15359
[35] Hu L, Cheng F, Tang Y and Wang H 2021 *Euro. Phys. J. B* **94** 8
[36] Wang Y, Wang Z, Wang Q, Zhou S, Han Q, Gao W, Ren K, Qi J and J Dong 2019 *J. Phys. Chem. C* **123** 24754
[37] Stauber T, Low T and Gomez-Santos G 2020 *Nano Lett.* **20** 8711
[38] Tang Y and Cohen A E 2010 *Phys. Rev. Lett.* **104** 163901
[39] Horrer A, Zhang Y, Gerard D, Beal J, Kociak Plain M J and Bachelot R 2020 *Nano Lett.* **20** 509
[40] Hu L, Xi F, Qv L and Fang Y 2018 *ACS Omega* **3** 1170
[41] Schäferling M, Yin X and Giessen H 2012 *Opt. Expres* **20** 26326